Rotational Magnetic Moments of the Alkali Molecules*

R. A. BROOKS, C. H. ANDERSON,† AND N. F. RAMSEY
Harvard University, Cambridge, Massachusetts
(Received 14 May 1964)

The rotational magnetic moments of the diatomic alkalis have been measured by the molecular-beam magnetic-resonance method. The values obtained for the gyromagnetic ratios g_J (in nm) are: Li_2, 0.10797; Na_2, 0.03892; K_2, 0.02162; Rb_2, 0.00953; Cs_2, 0.00547. The effect of the electric quadrupole interaction on the resonance is investigated, and found to lead to a slight broadening, but, in the limit of high J, to no displacement. An interpretation of the results in terms of the irrotational-flow model used by Espe for hydrogen is given.

I. INTRODUCTION

UNTIL recently, measurements of magnetic moments by the molecular-beam resonance method have been primarily concerned with nuclear magnetic moments in $^1\Sigma$ molecules, or electronic moments in paramagnetic atoms. There is a third type of magnetic moment which can exist in molecules; namely, that due to the rotation of the molecule as a whole, and measurements of this quantity are of value in the study of molecular structure. Although the rotational moment of hydrogen was measured by the molecular beam technique in 1939,[1] for the next twenty years no other rotational moments were studied in this way because other molecules, being heavier, have correspondingly lower gyromagnetic ratios, and it was feared that, assuming a single quantum transition ($\Delta m_J = \pm 1$), the changes in deflection would be too small.

However, recent experiments[2–4] in this laboratory have demonstrated that small gyromagnetic ratios can be measured, for molecules with sufficiently large angular momenta, by producing a succession of transitions, i.e., by rotating the molecule through large angles. The net change in magnetic moment is accordingly large, and the deflections can then be detected. Thus it is now possible to pursue the natural continuation of the original experiments on hydrogen, by studying the structurally similar diatomic alkalis.

The quantity of interest is the gyromagnetic ratio, defined by $g_J = \mu_J/\mu_N J$, where μ_J is the rotational magnetic moment, μ_N is the nuclear magneton, and J is the rotational angular momentum quantum number.

The apparatus is described briefly in Sec. II with emphasis on the innovations made for this experiment. In Sec. III we present the results, including a discussion of the sign determination done on the lithium molecule. The effect of the quadrupole interaction is investigated in Sec. IV, and a statistical analysis of the resonance shape is performed using the fact that, at the temperatures used in the experiments, high J values are excited. Finally, in Sec. V we discuss the significance of the results, in terms of the structural relationship of the alkalis to hydrogen.

II. APPARATUS

The molecular-beam machine used in these experiments was originally built by Kolsky *et al.*[5] specifically for the purpose of doing high-precision work on hydrogen, and has subsequently been modified by other workers. Its outstanding feature is a C magnet 150 cm long, resulting in a resonance width in the hydrogen work of as little as 300 cps, although in the present experiment no more than a 12-in. length of the magnet has been used. We will describe here only the apparatus changes that have been made for the present work.

A. Ovens

The ovens used are a conventional type, made of stainless steel, and heated by coils of 12-mil tantalum wire. The loading hole is sealed by a threaded plug ($\frac{9}{16}$ in.$\times$27) which screws down onto a flat ledge, with a nickel gasket being used to make the seal. This method has proved more convenient to use than the former method of making a force fit with a tapered steel plug. The beams were formed by loading the oven with about 0.3 g of pure metal, and heating to a temperature sufficient to produce about 1-mm vapor pressure. In the case of rubidium and cesium, which are supplied in evacuated glass ampules, the end of the ampule containing the metal was broken off and placed directly in the oven, glass and all.

B. Detector

In the earlier detector,[3] a hot tungsten wire had been used to ionize the beam. However, the alkali impurities present in the tungsten created a large background that made delicate measurements difficult. This difficulty has appeared only in recent years, and is apparently

* Supported in part by the U. S. Office of Naval Research and the National Science Foundation.
† Present address: RCA Research Laboratory, Princeton, New Jersey.
[1] N. F. Ramsey, Phys. Rev. **58**, 226 (1940).
[2] M. R. Baker, C. H. Anderson, J. Pinkerton, and N. F. Ramsey, Bull. Am. Phys. Soc. **6**, 19 (1961).
[3] T. R. Lawrence, C. H. Anderson, and N. F. Ramsey, Phys. Rev. **130**, 1865 (1963).
[4] J. W. Cederberg, C. H. Anderson, and N. F. Ramsey, Bull. Am. Phys. Soc. **8**, 327 (1963).
[5] This machine is described in detail in the book, N. F. Ramsey, *Molecular Beams* (Oxford University Press, New York, 1956).

due to changes in the methods for processing tungsten. We decided to try an iridium filament, in the hope of reducing the background. The iridium wire, 0.001 in. in diameter, was ordered from the Sigmund Cohn Corporation, and has worked out very satisfactorily. After heating the wire for several hours at a high temperature (120 mA) to remove the surface contamination, the background was found to be negligible. It has been found that the tension on the filament must be kept very light, just sufficient to keep it straight, as otherwise it will break.

The ions coming off the hot wire are accelerated, passed through a mass spectrometer, and focused onto the first dynode of an electron multiplier having a current gain of about 30 000. The output current is passed through a resistance of $10^9\,\Omega$, and the voltage across the resistance is measured by an electrometer. During a resonance sweep, the rf current is on-off modulated at 16 cps, and the resulting ac signal is measured by a lock-in detector with a 23-sec time constant, and displayed on a recorder.

C. rf Equipment

When the experiment was begun, there were two rf coils in the machine[6]: a $1\frac{1}{2}$-in. coil for producing a rotating magnetic field for use in sign determination, and a 12-in. coil. Neither coil had sufficient turns to produce the strong oscillating fields necessary for detecting weak g values, so a new coil was constructed, replacing the old 12-in. coil.

The new coil is actually two coils mounted on the same flange. One coil is 12 in. long and consists of 72 turns of water-cooled copper tubing. Taps are taken off at 1 in. and 4 in., so that a variety of lengths is available. Wound around the center of this coil is another one, 3 in. long, consisting of 250 turns of No. 22 enameled copper wire, with a center tap. This arrangement was designed so that cooling for the 3-in. coil could be obtained by circulating water through the long coil.

The inductances of the coils are approximately 2 μH for the 12-in. one, and 100 μH for the 3-in. one. The long coil is usually driven directly from the amplifier, its impedance being approximately one ohm at 100 kc/sec. The short coil, on the other hand, has an impedance of 20 Ω at 25 kc/sec, and the current through it can be appreciably increased by tuning with a series capacitor, even at very low frequencies.

The power amplifier used for most of the rotational moment measurements was a McIntosh MC–275 amplifier. This amplifier is rated at 150 W up to 60 kc/sec, at 75 W up to 100 kc/sec, and produces a usable output at 300 kc/sec. It also has the advantage of providing a variety of output impedances. The amplifier was driven by an inexpensive RC oscillator.

Cederberg[7] has carried out a numerical calculation, in the limit of high J, for the observed resonance curve for a rotational moment with no internal interactions. He found that the rf field which produces the maximum resonance signal is given by the same expression as is obtained for a nuclear resonance on a spin-$\frac{1}{2}$ nucleus. If the field is created by a current I (rms) flowing in a solenoidal coil of N turns, the expression may be written

$$NI_{\rm opt}=(11.4/g)(T/M)^{1/2}, \tag{1}$$

where T is the source temperature in °K and M is the molecular weight.

In our case, the quadrupole interaction greatly complicates the calculation, but it appears likely that the optimum rf current should be close to that given by Eq. (1).

In Table I values of the optimum rf current are calculated from the above equation, using the experimentally determined g values. Also listed are the current levels attained in practice at a typical set of frequencies. Finally, for completeness, we display some typical characteristics of the beams.

TABLE I. rf levels and beam deflections. $I_{\rm opt}$ is the optimum rf current calculated from Eq. (1), while $I_{\rm prac}$ represents typical current levels attained in practice. T is the oven temperature, α is the most probable velocity $[\alpha=(2kT/m)^{1/2}]$, J_m is the most probable angular momentum, and s is the average deflection at the detector, assuming an optimum rf field, for molecules with velocity α and angular momentum J_m.

	$I_{\rm opt}$ (A)	$I_{\rm prac}$ (A)	T (°K)	α (10^4 cm/sec)	J_m	s (10^{-3} in.)
Li^7_2	13.0	6.4	1100	11.4	24	1.38
Na^{23}_2	16.2	12.7	715	5.0	41	1.28
K^{39}_2	21.6	7.1	645	3.7	63	1.20
Rb^{85}_2	8.8	4.5	570	2.2	95	0.91
Cs^{133}_2	11.6	5.4	515	1.8	121	0.73

III. RESULTS

Some typical resonance curves are shown in Fig. 1, and a complete tabulation of data is given in Table II. The magnetic fields H_0 were calibrated by observing nuclear resonances in the molecules. The rotational resonances were then performed, and the g values were found from the central resonance frequency ν_0, using the relation

$$g_J=h\nu_0/H_0\mu_N. \tag{2}$$

One interesting feature of these results is that the rotational moments obtained are approximately equal to the moment of hydrogen multiplied by the inverse ratio of the masses, as is evidenced by the last column

[6] Although frequencies as low as 13 kc/sec have been used, it will be convenient to follow conventional usage and refer to the transition-inducing field, in general, as radio frequency (rf).

[7] J. W. Cederberg (to be published).

TABLE II. Experimental results. For those runs indicated by asterisks, the field calibrations are uncertain by several percent because of hysteresis effects in the magnets. In all other cases the accuracy of field calibration is better than that of the frequency determination. The best values of g_J are taken only from the runs made with an accurately calibrated field, weighted according to the number of runs in each group and their signal-to-noise ratio. The estimated uncertainty in the last decimal place is given in parentheses. The last column gives values of g_J of hydrogen multiplied by the ratio of the alkali mass to that of hydrogen.

	H_0 (G)	ν_0 (kc/sec)	g_J (nm)	g_J (best value) (nm)	$g_J(H_2) \times (M/M_{H_2})$ (nm)
$Li^7{}_2$	646*	50.0	0.10154*	0.10797(11)	0.12677
	1350.6*	107.9	0.10480*		
	1350.6	111.16	0.10797		
$Na^{23}{}_2$	646*	18.9	0.03838*	0.03892(10)	0.03868
	3239	95.7	0.03876		
	3021.4	90.01	0.03908		
$K^{39}{}_2$	1350.6*	21.85	0.02122*	0.02163(6)	0.02283
	2931.8	48.35	0.02163		
	3021.4	49.83	0.02163		
$Rb^{85}{}_2$	1350.6*	10.0	0.00971*	0.00953(4)	0.01047
	3241	23.38	0.00946		
	3230	23.47	0.00953		
$Rb^{85}-Rb^{87}$	3230	23.14	0.00940	0.00940(6)	
$Cs^{133}{}_2$	3232	13.3	0.00540	0.00547(3)	0.00669
	3225	13.5	0.00549		

of Table II. This point will be examined in more detail in Sec. V.

A special note should be given about lithium, potassium, and rubidium, for each of which there are two naturally occurring isotopes. Although the mass spectrometer was usually set for the most abundant isotope, the hybrid molecules were still detected. That is, for lithium, 7.4% of the signal was due to Li^7-Li^6; for potassium, 6.9% was due to $K^{39}-K^{41}$, and for rubidium, 28% was due to $Rb^{85}-Rb^{87}$. In the case of rubidium and potassium, the resonant frequency of the hybrid molecule is so close to that of the homonuclear molecule, that the two are not resolved into separate peaks. The resonance frequencies for $Rb^{85}-Rb^{85}$ and $K^{39}-K^{39}$ have been obtained from the experimental curves by applying a small calculated correction of approximately 0.05 kc/sec in each case. In the case of lithium, the resonant frequency of Li^7-Li^6 is 7% higher than that of $Li^7{}_2$, and this is far enough off the central peak so that it shows up as a slight bump on the high-frequency side (see Fig. 1). Also included in Table II are several runs taken with the mass spectrometer set for mass 87, to obtain the rotational moment of $Rb^{85}-Rb^{87}$.

Although the structural similarity of the alkali molecules and hydrogen (see Sec. V) suggests that the signs of the measured moments should be the same as for hydrogen, i.e., positive, it still is desirable to measure the sign of at least one alkali moment. As mentioned earlier, there was already in the machine a coil for producing rotating magnetic fields, for use in sign determinations. It consists of two coils at right angles to each other, so that if the currents in each coil are of equal magnitude, but out of phase by 90°, a rotating field is produced. Now since each coil has only four turns, it would be impossible with the existing rf equipment to produce sufficiently strong fields for observing weak g values. Accordingly, we decided to do the sign determination on lithium, which has the largest g value of the alkalis.

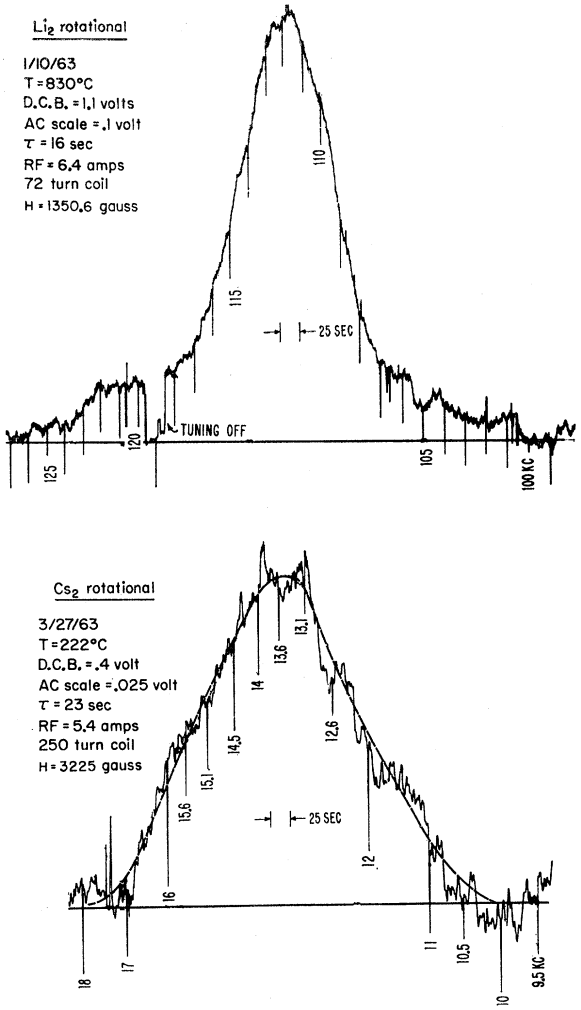

FIG. 1. Resonance curves for Li_2 and Cs_2.

A simple RC phase shifter was used to provide the 90° phase shift, with the McIntosh amplifier used in its stereo mode, driving the two coils separately. The experiment consisted of applying a rotating field at the resonance frequency, then reversing the sense of rotation, and observing which sense produced a resonance signal. The sign of the moment may then be determined, since the field is only effective when rotating in the direction of the magnetic moment precession. The sign was found to be positive, as had been expected.

TABLE III. Values of κ.

$I=\frac{3}{2}$			$I=\frac{5}{2}$				$I=\frac{7}{2}$			
$\lvert m_1\rvert$ \ $\lvert m_2\rvert$	$\frac{3}{2}$	$\frac{1}{2}$	$\lvert m_1\rvert$ \ $\lvert m_2\rvert$	$\frac{5}{2}$	$\frac{3}{2}$	$\frac{1}{2}$	$\lvert m_1\rvert$ \ $\lvert m_2\rvert$	$\frac{7}{2}$	$\frac{5}{2}$	$\frac{3}{2}$	$\frac{1}{2}$
$\frac{3}{2}$	1	0	$\frac{5}{2}$	1	$\frac{2}{5}$	$\frac{1}{10}$	$\frac{7}{2}$	1	$\frac{4}{7}$	$\frac{2}{7}$	$\frac{1}{7}$
$\frac{1}{2}$	0	-1	$\frac{3}{2}$	$\frac{2}{5}$	$-\frac{1}{5}$	$-\frac{1}{2}$	$\frac{5}{2}$	$\frac{4}{7}$	$\frac{1}{7}$	$-\frac{1}{7}$	$-\frac{2}{7}$
			$\frac{1}{2}$	$\frac{1}{10}$	$-\frac{1}{2}$	$-\frac{4}{5}$	$\frac{3}{2}$	$\frac{2}{7}$	$-\frac{1}{7}$	$-\frac{3}{7}$	$-\frac{4}{7}$
							$\frac{1}{2}$	$\frac{1}{7}$	$-\frac{2}{7}$	$-\frac{4}{7}$	$-\frac{5}{7}$

IV. EFFECT OF QUADRUPOLE INTERACTION

A. Energy Levels

If there were no internal interactions, the resonance curves would simply contain one spike at the resonant frequency given by Eq. (2). However, in addition to the interaction of μ_J with the external field H_0, there exist also the interactions with the nuclei; namely, the spin-rotational and electric quadrupole interactions.[8]

The first of these is small in the alkali molecules and will be neglected. The electric quadrupole interaction for a diatomic homonuclear molecule is described by the Hamiltonian[9]

$$\mathcal{H}_q=\frac{-eqQ}{I(2I-1)(2J-1)(2J+3)}\times\tfrac{1}{6}\sum_{ij}[\tfrac{3}{2}(I_iI_j+I_jI_i)_1+\tfrac{3}{2}(I_iI_j+I_jI_i)_2-2\delta_{ij}I(I+1)]\times[\tfrac{3}{2}(J_iJ_j+J_jJ_i)-\delta_{ij}J(J+1)],$$

where Q is the quadrupole moment of either nucleus, q is the field gradient along the internuclear axis, I is the nuclear spin, and the subscripts 1 and 2 refer to the first and second nucleus, respectively.

The complete Hamiltonian is

$$\mathcal{H}=\boldsymbol{\mu}_J\cdot\mathbf{H}_0+(\boldsymbol{\mu}_1+\boldsymbol{\mu}_2)\cdot\mathbf{H}_0+\mathcal{H}_q,$$

where μ_1 and μ_2 are the magnetic moments of the nuclei. For the conditions of this experiment, $\mathcal{H}_q$ is small compared to the other terms, so a perturbation approach is justified. We start out with a strong field representation, with stationary states described by the quantum numbers I_1, I_2, J, m_1, m_2, and m_J. However, for identical nuclei with half-integral spins, symmetry principles require that the stationary states be taken as

odd J:

$$\frac{1}{\sqrt{2}}|m_1m_2\rangle+\frac{1}{\sqrt{2}}|m_2m_1\rangle \quad (m_1\neq m_2)$$

$$|m_1m_2\rangle \quad (m_1=m_2)$$

even J:

$$\frac{1}{\sqrt{2}}|m_1m_2\rangle-\frac{1}{\sqrt{2}}|m_2m_1\rangle \quad (m_1\neq m_2).$$

For simplicity, we will use the notation $|(m_1m_2)\rangle$ to refer to these symmetrized or antisymmetrized states.

From first-order perturbation theory, the energy levels are given by

$$\langle\mathcal{H}\rangle=g_J\mu_Nm_JH_0+g_I\mu_N(m_1+m_2)H_0+\langle(m_1m_2)m_J|\mathcal{H}_q|(m_1M_2)m_J\rangle.$$

The matrix elements of $\mathcal{H}_q$ have already been worked out[9]; we need only take into account the use of symmetrized states here. The result is, for the diagonal matrix elements,

$$\langle(m_1m_2)m_J|\mathcal{H}_q|(m_1m_2)m_J\rangle=\frac{-eqQ}{2(2J-1)(2J+3)}\kappa[3m_J^2-J(J+1)],$$

where

$$\kappa=[\tfrac{3}{2}(m_1^2+m_2^2)-I(I+1)]/I(2I-1).$$

The factor κ refers to the spin state of the nuclei, and is never greater than one. Values of κ are listed in Table III for the spins involved in the present experiment. Note that for spin $\frac{3}{2}$, in half the molecules the value of κ is zero, because the quadrupole interaction with one nucleus cancels that with the other.

For a transition $m_J\rightarrow m_J-1$, the change in m_J^2 is $\Delta m_J^2=2m_J-1$, so that the frequency required for the

[8] The effect of the quadrupole interaction on nuclear transitions has been calculated previously [(B. T. Feld and W. E. Lamb, Phys. Rev. **67**, 15 (1945); H. M. Foley, *ibid.* **71**, 747 (1947)], but not its effect on rotational transitions.

[9] See, for example, Ref. 5, Appendix C.

transition, equal to the energy difference divided by h, is easily seen to be

$$\nu=\nu_0+\nu',$$

where ν_0 is given by Eq. (2), and

$$\nu'=\nu-\nu_0=\frac{-3eqQ/h}{2(2J+3)}\,\kappa\,\frac{2m_J-1}{2J-1}. \tag{3}$$

Three comments should be made about this expression. First, the frequency for a transiton depends on m_J, and hence is different for successive transitions. This means that the resolving power of the rf coil cannot be too great, or multiple quantum transitions will be hindered. Second, the effect of the quadrupole interaction is diminished by a factor of approximately $1/J$. This corresponds physically to the fact that in a $\Delta m_J=\pm1$ transition, for large J, the relative orientation of the nuclei and the rotational angular momentum is changed very little. Third, the quadrupole contribution, in first order, is symmetrical about the central resonance frequency ν_0.

Although the above expression is sufficient for our purposes, it is interesting to carry the calculation to second-order perturbation theory. The result is that a term ν'' must be added to the frequency given above, where

$$\nu''=\frac{3eqQ/h}{2(2J+3)}\,\frac{3eqQ}{8(g_I-g_J)\mu_N H_0}\,\frac{1}{(2J+3)(2J-1)^2}$$
$$\times\{-(2x-1)[(J+\tfrac{1}{2})^2-2x^2+2x-1]M_1+(2x+1)[(J+\tfrac{1}{2})^2-2x^2-2x-1]M_2$$
$$+[(x-1)/8][(J+\tfrac{1}{2})^2-x^2+2x-1]M_3-[(x+1)/8][(J+\tfrac{1}{2})^2-x^2-2x-1]M_4\},$$

where

$$x=m_J-\tfrac{1}{2},$$

and the M's are complicated factors referring to the spin state of the nuclei, with magnitudes on the order of one. The important feature of this result is that, in addition to a further broadening of the resonance, there is also an asymmetry introduced, due to the fact that the brackets in the above equation contain some terms even in x. However, the magnitude of the asymmetry is small, since the even terms are cut down by an additional factor of $1/J$.

B. Statistical Analysis

Since the molecules are at high temperatures, with large J values present, we do not observe single lines, but rather a large number of unresolved lines. Thus a statistical analysis, making use of the fact that $J\gg1$, is appropriate. We are interested in knowing the signal intensity $I(\nu)$, where $I(\nu)d\nu$ represents the number of molecules per second undergoing transitions for an oscillating field with frequency between ν and $\nu+d\nu$. We assume that all transitions will be detected if the corresponding frequency lies in the interval $d\nu$. Thus we neglect such effects as coil "broadening" and detection probabilities. This corresponds to an idealized apparatus with a very narrow, rectangular frequency "window," and very narrow slits.

The contribution from molecules of a given J, $I(\nu,J)$, is equal to the density of m_J states in the frequency interval $d\nu$,

$$\left|\frac{dm_J}{d\nu}\right|=\begin{cases}\dfrac{(2J-1)(2J+3)}{3\kappa|eqQ|/h} & \left(|\nu-\nu_0|<\dfrac{3|eqQ|/h}{2(2J+3)}\kappa\right)\\ 0 & \text{(elsewhere)}\end{cases}$$

multiplied by the number of molecules in each m_J state,

$$N=Ce^{-a^2J(J+1)},$$

where C is a normalization constant and $a^2=h^2/2kT\mathcal{I}=\frac{1}{2}J_m^2$, where $\mathcal{I}$ is the moment of inertia and J_m the

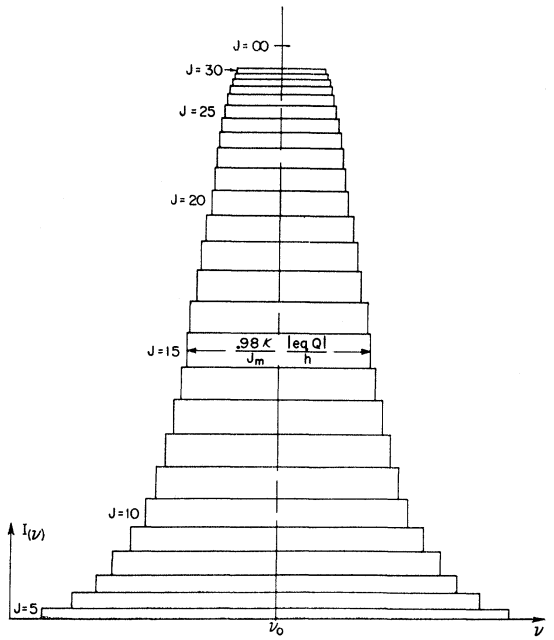

FIG. 2. The contribution of each J state to the total intensity is illustrated for a system with $J_m=10$. The low J states don't contribute much because there are few m_J levels in a given frequency range, while the high J states don't contribute much because, although the levels are close-spaced, their populations are small. The largest contribution comes from $J=\sqrt{2}J_m$, or, in this case, $J=14$.

most probable angular momentum. Thus

$$I(\nu,J)=hC(3\kappa|eqQ|)^{-1}(2J-1)(2J+3)e^{-a^2J(J+1)}.$$

In Fig. 2, $I(\nu,J)$ is plotted for values of J from $J=5$ on up, for a system with a most probable angular momentum of 10.

The total signal intensity $I(\nu)$ is obtained by summing over all the J states that can contribute at the frequency ν (see Fig. 2). The lower limit may be taken as $J=0$,[10] while the upper limit $J_{\max}$ is obtained from Eq. (3) by setting $m_J=J$, yielding

$$J_{\max}(\nu)=\left|\frac{3eqQ/h}{4(\nu-\nu_0)}\right|\kappa-\tfrac{3}{2}.$$

Thus the desired expression is, using the approximation $J\gg1$,

$$\begin{aligned}I(\nu)&=4hC(3\kappa|eqQ|)^{-1}\int_0^{J_{\max}}J^2e^{-a^2J^2}dJ\\&=2hC(3\kappa|eqQ|a^3)^{-1}[\tfrac{1}{2}\pi^{1/2}\operatorname{erf}(aJ_{\max})\\&\qquad-aJ_{\max}\exp(-a^2J_{\max}{}^2)].\end{aligned}\quad(4)$$

Equation (4) gives the shape of the resonance curve for a given value of κ. It corresponds to a smooth envelope of the curve shown in Fig. 2. From Eq. (4) we find that the full width of the curve at half-height is given by

$$\Delta\nu_{\text{quad}}=0.98(\kappa/J_m)(|eqQ|/h).\quad(5)$$

C. Comparison with Experimental Curves

There are a number of difficulties in comparing Fig. 2 with the experimental curves. First of all, Fig. 2 gives the resonance shape for only one state of the nuclear spins, specified by a given value of κ. The actual curve will be a superposition of curves for the various κ values. Curves for small κ will be tall and thin; those for large κ will be short and fat. The shape of the resulting curve will not be simple.

Secondly, the resonance shape illustrated in Fig. 2 is that which would be observed in an apparatus with infinite resolving power. In an actual apparatus there is a certain "coil width," due to the finite time spent in the rf region. Indeed, as we have seen, this coil width is necessary in order that successive quantum transitions may occur.

The question of what is the coil width is more complicated here than for the more familiar case of a system with only two states, for which we have[11]

$$\Delta\nu_{\text{coil}}=1.2\alpha/l,\quad(6)$$

where $\Delta\nu_{\text{coil}}$ is the full width at half-height for a δ-function resonance. In deriving the above equation, it is assumed that all transitions will be detected. In our case, however, the probability of detection depends on the degree of deflection, and hence depends on the J value as well as on the velocity.

To investigate this effect, we must look at each J value individually. Qualitatively we can see that the low J states will be very much suppressed, since they can not undergo large deflections. As we approach $J=J_m$, the deflections will increase to a detectable amount (see Table I), and the signal intensity will approach the full value illustrated in Fig. 2. As we go on to higher J values, the signal intensity will remain at the levels shown in Fig. 2, but the width will now increase beyond that illustrated, due to the increased coil broadening, (i.e., since, for large J, less rotation is required for detection, frequencies farther off resonance can still produce a signal).

We could use the above approach to obtain an approximate resultant curve, but it would not be very informative, since it results from a complicated interplay between the quadrupole shape as derived in Sec. B above, the effect of the spin states of the nuclei, the broadening effects of the coil, and the varying detection probabilities. It is quite clear, for example, that an accurate verification of the quadrupole constants is impossible. Therefore, we shall content ourselves with simply comparing the widths of the experimental curves with the quadrupole widths as given by Eq. (5), taking $\kappa=\frac{1}{2}$ as an average value of κ and using the values of eqQ obtained by Logan *et al.*[12]; and also with the coil widths given by Eq. (6), which is probably approximately valid in the present case. This is done in Table IV.

TABLE IV. Resonance widths—experimental versus theoretical.

	$\lvert eqQ/h\rvert$ (kc/sec)	$\Delta\nu_{\text{quad}}$ (kc/sec)	$\Delta\nu_{\text{coil}}$ (kc/sec)	$\Delta\nu_{\text{exp}}$ (kc/sec)
Li_2	60	1.2	4.4	5.9
Na_2	423	5.1	1.9	6.8
K_2	158	1.2	1.4	2.5
Rb_2	1100	5.7	3.5	6.0
Cs_2	230	0.9	2.9	3.4

The agreement turns out to be better than would be expected, considering the approximations involved. In the two cases where the quadrupole width is the dominant factor (Na_2 and Rb_2), the experimental width is just slightly greater than the predicted quadrupole width. And in the two cases where the coil broadening is dominant (Li_2 and Cs_2), the experimental width is somewhat greater than the predicted coil width.

[10] Although the statistical treatment is not valid for low J states, their contribution is so small that the error is negligible.

[11] Reference 5, p. 124.

[12] R. A. Logan, R. E. Cote, and P. Kusch, Phys. Rev. 86, 280 (1952).

V. INTERPRETATION

In 1956, Espe[13] obtained good agreement with theory for the rotational moment of hydrogen, using an irrotational flow model coupled with a variational technique of calculation. Using the simplest suitable trial function, he found for the electronic contribution to the g value

$$g_e=\frac{1}{MR^2}\langle x^2+y^2\rangle\left(\frac{\langle x^2-y^2\rangle}{\langle x^2+y^2\rangle}\right)^2, \tag{7}$$

where x and y are the electron coordinates perpendicular to the axis of rotation, and M and R are the mass (in amu) and radius of the nuclei. The significance of the various factors in the above equation is as follows. The $1/MR^2$ factor arises because the rotational velocity of the nuclei depends inversely on their moment of inertia. The $\langle x^2+y^2\rangle$ factor arises because the effectiveness of each electron in creating a magnetic moment depends on the square of its distance from the axis. Finally, the last factor arises because the amount of rotation imparted to the electrons by the nuclei depends on the asymmetry of the electron cloud, measured in this approximation by the "normalized quadrupole moment," $\langle x^2-y^2\rangle/\langle x^2+y^2\rangle$.

Although an accurate interpretation of our experimental results would make use of calculated wave functions, we can gain some understanding of them by noticing the similarity of the structure of the alkalis to that of hydrogen. Each nucleus is surrounded by one or more closed electron shells whose only effect, neglecting their polarizations, is to reduce the effective charge of the nucleus. Thus, to a good approximation, the alkali molecule consists of two ions with charge e and mass M, with the two remaining valence electrons performing an orbit around the entire molecule. This is the same structure as hydrogen.

It is therefore convenient to break the g value up into the contribution of the ions g_i, and that of the valence electrons g_e. Now g_i is simply equal to M_p/M nuclear magnetons, where M_p is the proton mass, so experimental values of g_e can be obtained by subtracting g_i from the measured g values. These quantities are listed in Table V, with data on hydrogen included.[14]

TABLE V. Electronic contributions to magnetic moments.

	M (amu)	g_i (nm)	g_e (nm)	Mg_e
H_2	1.00758	1.00000	−0.11709	−0.118
Li_2	7.01763	0.14358	−0.03561	−0.250
Na_2	22.9957	0.04382	−0.00490	−0.113
K_2	38.973	0.02585	−0.00423	−0.165
Rb_2	84.95	0.01186	−0.00233	−0.198
Cs_2	132.91	0.00758	−0.00211	−0.280

The interesting feature of the experimental values of g_e is that the primary variation is as $1/M$. This is illustrated in the last column of Table V, where values of Mg_e are listed. Notice that after multiplying g_e by M, the total variation among the values is approximately a factor of 2, whereas before there was a variation by a factor of 56. This is what we would expect from Eq. (7), since we know that, for the alkalis, the quantities $\langle x^2+y^2\rangle/R^2$ and $\langle x^2-y^2\rangle/\langle x^2+y^2\rangle$ do not vary greatly. Further, since the degree of asymmetry in the electron cloud should diminish if its average radius increases faster than the internuclear distance, the effect of these two quantities should be in opposite directions.

The experimental values do deviate from a $1/M$ dependence, the general trend being that g_e does not decrease as rapidly as $1/M$. This deviation is due partly to the variations that do exist in the two factors mentioned above, but we must also remember that the approximations used in the derivation of Eq. (7) are not rigorously valid. In particular, we have neglected the asymmetry of the inner electron shells, which will, in fact, increase the electronic magnetic moment. Since this effect would be greater in larger molecules, it could account in large part for the observed deviations from $1/M$.

[13] I. Espe, Phys. Rev. 103, 1254 (1956).

[14] N. J. Harrick and N. F. Ramsey, Phys. Rev. 88, 228 (1952).